Rodríguez-Martínez, J.A. Fernández-Sáez, J., Zaera, R. (2015). The role of constitutive relation in the stability of hyper-elastic spherical membranes subjeted to dynamic inflation. International Journal of Engineering Science, 93, pp. 31-45.

DOI: https://doi.org/10.1016/j.ijengsci.2015.04.004

The role of constitutive relation in the stability of hyper-elastic spherical membranes subjected to dynamic inflation

Abstract

In this work the mechanical response of hyper-elastic spherical membranes subjected to dynamic inflation is revisited. Specifically, a comprehensive analysis on the role that the constitutive behaviour of the material has on the mechanical stability of the membrane has been developed. Six different strain-energy functions, frequently used to approximate the constitutive behaviour of elastomeric solids, have been considered: three of the Mooney-Rivlin class and three of the Ogden class. For all the constitutive models used, the material parameters have been obtained from Bucchi and Hearn (2013a,b), where the same set of experimental results was used to calibrate the models. We show that essential features of the dynamic response of the spherical shell are closely related to the strain-energy function selected to describe the constitutive behaviour of the membrane. As reported by Bucchi and Hearn (2013a,b), this issue is frequently overlooked within the literature since too often only one strain-energy function is used to address this type of dynamic problems.

Keywords:

Spherical membrane, Dynamics, Mechanical stability, Hyper-elasticity, Strain-energy function

1. Introduction

Since the pioneering works of Mooney (1940), Treolar (1944, 1949) and Rivlin (1948, 1996), the mechanics of hyper-elastic membranes under finite deformations has been a matter of great interest for the continuum mechanics community. The contributions to this topic over the last 70 years are by far too numerous to be cited individually. We focus here the attention on the (approximately) last decade, in which significant advances have been made on the investigation of the mechanical stability of inflated elastomeric shells. As described by Tamadapu and DasGupta (2013) and Kumar and DasGupta (2013), hyper-elastic inflated structures are used in modern applications such as in balloons, self-deploying structures, terrestrial and space structures, airbags and suspensions for cushioning and absorbing shocks. Moreover, we find an important application within the framework of biomedical engineering since the inflation of spherical and cylindrical

hyper-elastic shells is frequently taken as a canonical problem to investigate the formation and growth of saccular and fusiform aneurysms (Shah and Humphrey, 1999; David and Humphrey, 2003; Haslach and Humphrey, 2004; Volokh and Vorp, 2008; Freitas, 2009; Rodríguez and Merodio, 2011; Alhayani et al., 2014). In this regard, one should pay special attention to the papers of Fu and co-workers (Fu et al., 2008; Pearce and Fu, 2010; Fu and Xie, 2010; Il'ichev and Fu, 2012, 2014; Fu et al., 2012; Fu and Xie, 2014) who focused on the analysis of bifurcated (bulged) configurations from pressurized tubular and spherical membranes, and explored the stability of the bulging motion. The authors stated that this bifurcation interpretation of the initial formation of aneurysms could provide a theoretical framework under which different mechanisms leading to aneurysms development can be assessed in a systematic manner (Fu and Xie, 2012).

Driven by the applications described above, several authors have attempted to shed light into the key role played by the constitutive behaviour of the membrane material on the mechanical response of the shell. One has to mention the work of Ogden et al. (2004) who carried out a systematic study on the procedure of *fitting of experimental data* which is regularly used to determine the material parameters of different hyper-elastic constitutive laws. Ogden et al. (2004) pointed out that the fitting process often leads to non-unique optimal parameters. The authors noted that, for a given constitutive model, to use different sets of material parameters markedly affects the solution of boundary value problems, despite these material parameters may be fitted using the same experimental data. With the aim of deepen into the interplay between the material parameters and the mechanical response of elastomeric membranes, Biscari and Omati (2010) studied the inflation of thin spherical shells modelled as a (generalized) Knowles' material (Knowles, 1977). By allowing the constitutive parameters to vary within a wide range of values, Biscari and Omati (2010) showed the close relation between the values assigned to the material parameters and the mechanical stability of the shell. Within the same framework, we highlight the very recent work of Mangan and Destrade (2015) who, as previously did Biscari and Omati (2010), revisited the inflation of spherical shells. Mangan and Destrade (2015) used the 3-parameter Mooney (Mooney, 1940) and the Gent-Gent (Pucci and Saccomandi, 2002) models to describe the membrane behaviour. The authors pointed out the constitutive sensitivity of the problem at hand and the great influence exerted by the material parameters on the stability/instability of the shell response.

Nevertheless, the work of Bucchi and Hearn (2013a,b) seems to be the only research paper which relies on a significant number of different strain energy functions to provide detailed analysis

on the interplay between the material constitutive model and the mechanical response of the membrane. It is pointed out by Bucchi and Hearn (2013b) that, in the recent literature, too often only one strain-energy function is used to describe the material behaviour. Even if two or more strain-energy functions are utilised, their parameters are frequently taken from different sources. This practice is a drawback as soon as different sources implies that different sets of experimental data have been used for determining the model parameters. Comparison of alternative analyses based on using different strain-energy functions requires that the parameters of these constitutive models have been obtained using a unique set of experiments and a common identification procedure.

With this in mind, we develop here an analytical study with the aim of exploring specifically the role played by the strain-energy function in the inflation of spherical shells. Unlike the work of Bucchi and Hearn (2013a,b), the constitutive sensitivity analysis developed in the present paper lies within the dynamic regime. While the dynamic inflation of elastomeric shells is less explored than the static one, it was shown by Verron et al. (1999, 2001) and Yuan et al. (2010) that inertia has a significant influence on the mechanical stability of spherical balloons. Within this framework, we address in this paper a key issue: different constitutive models calibrated using the same set of experimental data and the same fitting procedure provide different predictions of the dynamic response of the spherical balloon. This highlights how crucial may be the selection of the (appropiate) strain-energy function for (reliable) mathematical modelling of hyper-elastic membranes subjected to dynamic solicitations. As such, our investigation complements recent papers developed under similar premises but within the static regime, see (Biscari and Omati, 2010; Bucchi and Hearn, 2013a,b; Mangan and Destrade, 2015).

The paper is organized as follows. In Section 2 the equation which governs the dynamic inflation of the spherical membrane is deduced. Then, the two loading cases to be analysed are presented: a spherical membrane subjected to (1) constant inflation acceleration and (2) constant inflation pressure step. Section 3 shows the six different strain-energy functions, from which the constitutive relation is derived, that are selected to describe the membrane behaviour. Three constitutive models belong to the Mooney-Rivlin class (Rivlin, 1948) and the other three to the Ogden class (Ogden, 1972). These are *classical* models that have been frequently used in the literature to describe the mechanical behaviour of elastomeric solids. In section 4 results are presented and analysed combining, systematically, the two loading scenarios and the six constitutive equations. We point out that essential features of the dynamic response of the shell

are closely related to the strain-energy function selected to describe the membrane behaviour. Specifically, we focus the attention on the effect that material constitutive modelling has on the mechanical stability of the membrane. This issue is further discussed in section 5 where a critical overview of the main outcomes of this research is developed. Section 6 summarizes the key conclusions obtained from this investigation.

2. Problem formulation

2.1. Governing equation

Consider a spherical membrane of non-linear elastic, isotropic, and incompressible material of density ρ subjected to dynamic inflation. The membrane deformation is described in spherical coordinates (R, Θ, Φ) in the undeformed configuration, and (r, θ, ϕ) in the deformed configuration. Let (R_0, H_0) and (r_0, h_0) denote the membrane midsurface radius and thickness in the undeformed configuration and in the deformed configuration, respectively. Let $\sigma_{rr} = 0$ and $\sigma_{\theta\theta} = \sigma_{\phi\phi}$ be the diagonal components of the Cauchy stress tensor in the radial and circumferential (meridional and azimuthal) directions respectively. Because of the spherical symmetry, all the variables depend only on time t. The conservation of linear momentum in the radial direction leads to:

$$\rho h_0 \ddot{r}_0 = -2\sigma_{\theta\theta}\frac{h_0}{r_0} + p \tag{1}$$

where p is the inflation pressure and a superposed dot denotes differentiation with respect to time.

Let $\lambda_1 = h_0/H_0$ denote the principal stretch ratio in the thickness direction, and $\lambda_2 = \lambda_3 = \lambda = r_0/R_0$ be the principal stretch ratios in the circumferential directions. The incompressibility condition implies that $\lambda_1\lambda^2 = 1$. Then, we rewrite Eq. (1) as:

$$\rho H_0 R_0 \frac{\ddot{\lambda}}{\lambda^2} = -2\frac{\sigma_{\theta\theta}}{\lambda^3}\frac{H_0}{R_0} + p \tag{2}$$

Next, we introduce the following dimensionless variables:

$$\tau = \frac{t}{t_0}; \qquad \bar{\sigma} = \frac{\sigma_{\theta\theta}}{C_{10}^{M1}}; \qquad \bar{p} = p\frac{R_0}{C_{10}^{M1}H_0}$$

where $t_0 = R_0\sqrt{\frac{\rho}{C_{10}^{M1}}}$, being C_{10}^{M1} a material constant as further discussed in section 3.

Thus, Eq. (2) takes the following non-dimensional form:

$$\frac{\ddot{\lambda}}{\lambda^2} = -2\frac{\bar{\sigma}}{\lambda^3} + \bar{p} \tag{3}$$

where now a superposed dot denotes differentiation with respect to the dimensionless variable τ. Therefore, the problem gets reduced to solve an equation of the type:

$$\ddot{\lambda} = F\left(\lambda, \bar{p}\right) \tag{4}$$

with

$$F\left(\lambda, \bar{p}\right) = -\lambda^2 g\left(\lambda\right) + \lambda^2 \bar{p} \tag{5}$$

being $g\left(\lambda\right) = \frac{2\bar{\sigma}}{\lambda^3}$ a function which considers the non-linear elastic behaviour of the material. This function $g\left(\lambda\right)$ depends on the constitutive model used to describe the material behaviour as further shown in section 4.

2.2. Dynamic loading scenarios

We consider the case of the membrane initially in equilibrium and unstretched, i.e. subjected to the following initial conditions:

$$\lambda\left(0\right) = 1; \qquad \dot{\lambda}\left(0\right) = 0 \tag{6}$$

Then, two different dynamic loading scenarios are examined: (1) constant inflation acceleration and (2) constant inflation pressure step. One could argue that these loading scenarios do not reflect the complexity of the dynamic loading that has to be withstood by suspensions designed for cushioning and absorbing shocks or by aneurysms subjected to the sudden rise in blood pressure caused by automobile accidents or sports falls (see the introductory section). Nevertheless, we submit that the *idealized* loading scenarios we consider here can be assumed in the interest of further understanding the role played by the constitutive behaviour of the material on the dynamic response of the membrane, as further illustrated in section 4. These idealized loading scenarios are required to obtain closed analytical solutions, which help to interpret the outcomes of the analysis. Anyway, we cannot not deny that forthcoming studies of this type have to pay attention to different kinds of time-dependent loading scenarios which characterize the applications listed in the introductory section.

2.2.1. Case I: constant inflation acceleration

The governing equation can be written as:

$$\bar{p} = g\left(\lambda\right) + \frac{\ddot{\lambda}}{\lambda^2} \tag{7}$$

where the inflation pressure is an explicit function of the material constitutive behaviour $g\left(\lambda\right)$, the circumferential stretch λ and the constant acceleration $\ddot{\lambda}$. To be noted that if $\ddot{\lambda} = 0$ we obtain the static condition.

2.2.2. Case II: constant inflation pressure step

It is straightforward to demonstrate that:

$$\ddot{\lambda} = \frac{1}{2}\frac{d(\dot{\lambda}^2)}{d\lambda} \tag{8}$$

Therefore, from Eq. (4) we get:

$$\frac{d(\dot{\lambda}^2)}{d\lambda} = 2F\left(\lambda, \bar{p}\right) \tag{9}$$

Since $\bar{p}$ is independent of time, $\dot{\lambda}$ can be obtained as an explicit function of λ:

$$\dot{\lambda} = \pm\sqrt{2\int_1^{\lambda} F\left(\xi, \bar{p}\right) d\xi} \tag{10}$$

This expression allows to obtain the phase diagrams $\dot{\lambda}$ versus λ. Moreover, the temporal behaviour of the circumferential stretch is obtained as:

$$\tau = \frac{1}{\sqrt{2}}\int_1^{\lambda} \frac{d\zeta}{\sqrt{\int_1^{\zeta} F\left(\xi, \bar{p}\right) d\xi}} \tag{11}$$

To be noted that when the motion of the membrane is periodic (further discussions about the oscillatory response of the membrane are presented in section 4.2), the corresponding phase curve is a closed loop in the $(\lambda, \dot{\lambda})$ plane. Then, the dimensionless period T can be calculated as:

$$T = \sqrt{2}\int_1^{\lambda_{max}} \frac{d\zeta}{\sqrt{\int_1^{\zeta} F\left(\xi, \bar{p}\right) d\xi}} \tag{12}$$

where λ_{max} is the maximum value of the stretch in the oscillatory motion of the membrane.

3. Constitutive modelling

Hyper-elastic (also known as Green-elastic) materials are non-linear elastic materials for which the existence of a strain-energy function W can be postulated. The derivative of W with respect to a strain component determines the corresponding stress component, and therefore the material constitutive relation. Six different strain-energy functions are selected to describe the membrane behaviour. Three belong to the Mooney-Rivlin class (Rivlin, 1948) and the other three to the Ogden class (Ogden, 1972). The material parameters of the strain-energy functions are taken from Bucchi and Hearn (2013a,b), where the same set of experimental results (Treolar, 1944) was used to calibrate the models. Further, the same fitting procedure was followed to identify the material parameters of all the strain-energy functions considered (Bucchi and Hearn, 2013a,b). It can be easily checked that, despite they are not identical, the predictions of these 6 constitutive models within the linear limit are rather similar.

One could argue that these strain energy functions do not reflect the complexity of the *true* mechanical behaviour of elastomeric solids, whether they are structural or biological. In this regard, one could mention the paper of Hoo Fatt and Ouyang (2008) who showed the viscid behaviour of structural rubber-like materials within the dynamic regime, and the paper of Ogden and Saccomandi (2007) who pointed out the need of incorporating relevant biological information into the constitutive equations used to describe arterial walls. Nevertheless, we hold that the *simple* constitutive models studied in this paper facilitate the interpretation of the results which, in turn, enables to uncover essential features of the dynamic response of the shell. Namely, as further illustrated in section 4, it helps to show the key role that material constitutive modelling plays on the dynamic stability of the spherical membrane. On the other hand, in order to improve the description of the material behaviour, in future analyses we should not discard to incorporate additional material characteristics (like viscosity, compressibility, ...) in our mathematical modelling.

3.1. Mooney-Rivlin class

The Mooney-Rivlin class of models expresses the mechanical strain energy as:

$$W = \sum_i \sum_j C_{ij}^{Mk} (I_1 - 3)^i \, (I_2 - 3)^j \tag{13}$$

where $I_1 = \lambda_1^2 + \lambda_2^2 + \lambda_3^2$ and $I_2 = \lambda_1^2\lambda_2^2 + \lambda_2^2\lambda_3^2 + \lambda_1^2\lambda_3^2$ are the first and second invariants of the Green strain tensor. Moreover C_{ij}^{Mk} are material constants.

Three different models of the Mooney-Rivlin family (Treolar, 1944; Rivlin, 1948; Treolar, 1949; Yeoh, 1993), frequently used to approximate the constitutive behaviour of elastomeric solids (Wolters et al., 2005; Volokh and Vorp, 2008; Beatty, 2009; Bucchi and Hearn, 2013a,b), are considered:

- Neo-Hookean

$$W = C_{10}^{M1}(I_1 - 3) \tag{14}$$

Note that the parameter C_{10}^{M1} is directly related to the infinitesimal shear modulus of the material. Thus, with the aim of favoring the physical interpretation of our results, we selected in section 2 this parameter to define the dimensionless variables of our formulation.

- Mooney-Rivlin

$$W = C_{10}^{M2}(I_1 - 3) + C_{01}^{M2}(I_2 - 3) \tag{15}$$

- Yeoh

$$W = C_{10}^{M3}(I_1 - 3) + C_{20}^{M3}(I_1 - 3)^2 + C_{30}^{M3}(I_1 - 3)^3 \tag{16}$$

3.2. Ogden class

The Ogden class of models expresses the mechanical strain energy as:

$$W = \sum_{i=1}^{N} \frac{C_{i0}^{Ok}}{\alpha_i^{Ok}} \left(\lambda_1^{\alpha_i^{Ok}} + \lambda_2^{\alpha_i^{Ok}} + \lambda_3^{\alpha_i^{Ok}} - 3 \right) \tag{17}$$

where C_{i0}^{Ok} and α_i^{Ok} are material constants.

Three different models of the Ogden family (Ogden, 1972, 1997), frequently used to approximate the constitutive behaviour of elastomeric solids (Destrade et al., 2009; Volokh, 2011; Fu and Xie, 2012; Bucchi and Hearn, 2013a,b), are considered:

- Ogden N=1

$$W = \frac{C_{10}^{O1}}{\alpha_1^{O1}}\left(\lambda_1^{\alpha_1^{O1}} + \lambda_2^{\alpha_1^{O1}} + \lambda_3^{\alpha_1^{O1}} - 3\right) \tag{18}$$

- Ogden N=2

$$W = \frac{C_{10}^{O2}}{\alpha_1^{O2}}\left(\lambda_1^{\alpha_1^{O2}} + \lambda_2^{\alpha_1^{O2}} + \lambda_3^{\alpha_1^{O2}} - 3\right) + \frac{C_{20}^{O2}}{\alpha_2^{O2}}\left(\lambda_1^{\alpha_2^{O2}} + \lambda_2^{\alpha_2^{O2}} + \lambda_3^{\alpha_2^{O2}} - 3\right) \tag{19}$$

- Ogden N=3

$$W = \frac{C_{10}^{O3}}{\alpha_1^{O3}}\left(\lambda_1^{\alpha_1^{O3}} + \lambda_2^{\alpha_1^{O3}} + \lambda_3^{\alpha_1^{O3}} - 3\right) + \frac{C_{20}^{O3}}{\alpha_2^{O3}}\left(\lambda_1^{\alpha_2^{O3}} + \lambda_2^{\alpha_2^{O3}} + \lambda_3^{\alpha_2^{O3}} - 3\right) + \frac{C_{30}^{O3}}{\alpha_3^{O3}}\left(\lambda_1^{\alpha_3^{O3}} + \lambda_2^{\alpha_3^{O3}} + \lambda_3^{\alpha_3^{O3}} - 3\right) \tag{20}$$

4. Analysis and results

Following Ogden (1972), it can be easily shown that the expression for $\sigma_{\theta\theta}$ is given by:

$$\sigma_{\theta\theta} = 2\lambda\left(\lambda - \frac{1}{\lambda^5}\right)\left(\frac{\partial W}{\partial I_1} + \lambda^2\frac{\partial W}{\partial I_2}\right) \tag{21}$$

Previous expression is particularized for each strain-energy function considered, and inserted into $g(\lambda)$ to explore loading cases I (section 2.2.1) and II (section 2.2.2).

To be noted that, as shown by Janele et al. (1989), the spherical symmetry and the incompressibility of the material preclude the generation of wave disturbances in the problem at hand.

4.1. Constant inflation acceleration

Loading case I (section 2.2.1) is addressed. Firstly, the role of inflation acceleration on the response of the spherical membrane is examined.

4.1.1. Influence of inflation acceleration

Fig. 1 shows the dimensionless pressure $\bar{p}$ versus the circumferential stretch λ for several values of the acceleration $\ddot{\lambda}$. Three strain-energy functions are selected within those listed in section 3, namely: Ogden N=2 in Fig.1(a), Neo-Hookean in Fig.1(b) and Yeoh in Fig.1(c). These are chosen because they lead to three representative (distinct) behaviours for the static case (Beatty, 1987; Verron et al., 1999). The static condition is fulfilled considering in Eq. (7) that $\ddot{\lambda} = 0$:

- Ogden N=2 model: the static curve $\bar{p} - \lambda$ shows neither a maximum nor a minimum; increasing λ implies increasing $\bar{p}$. Eq. (7) becomes a bijection, for every inflating pressure $\bar{p}$ there is only one real root.

- Neo-Hookean model: the static curve $\bar{p} - \lambda$ shows a maximum which determines the greater pressure the membrane can withstand in static inflation. This is typically known as critical static pressure or limit pressure $\bar{p}^c$. For $0 < \bar{p} < \bar{p}^c$, Eq. (7) has two distinct real roots, one on the ascending portion of the curve and another on the descending portion. For $\bar{p} > \bar{p}^c$ there is not real solution for Eq. (7), the membrane cannot withstand such static pressure.

- Yeoh model: the static curve $\bar{p} - \lambda$ shows a local maximum $\bar{p}^{max}$ and a local minimum $\bar{p}^{min}$. The inflation curve consists on three branches, two stable and one unstable. For $0 < \bar{p} < \bar{p}^{min}$, Eq. (7) has only one real root in the first stable branch. For $\bar{p}^{min} < \bar{p} < \bar{p}^{max}$, Eq. (7) has three real roots, one in the first stable branch, one in the unstable branch and one in the second stable branch. For $\bar{p} > \bar{p}^{max}$, Eq. (7) presents only one real root in the second stable branch. To be noted that for $\bar{p} = \bar{p}^{min}$ and $\bar{p} = \bar{p}^{max}$ there are only two real roots.

Irrespective of the constitutive relation, increasing values of $\ddot{\lambda}$ lead to greater values of inflation pressure. Initial equilibrium of the membrane corresponds to $\bar{p} = \ddot{\lambda}$. Thus, the impact of acceleration on the inflation curve is maximum for $\lambda = 1$ and gets gradually reduced as λ increases, as can be deduced from Eq. (7). If $\lambda \to \infty$, virtually, the contribution of dynamic effects to the $\bar{p} - \lambda$ curve is negligible. Besides that, the shape of the inflation curves changes with $\ddot{\lambda}$. In this regard, some specific issues have to be commented:

- Ogden N=2 model: for $\ddot{\lambda} = 10$, $\ddot{\lambda} = 4$ and $\ddot{\lambda} = 2$ the inflation curve shows a local minimum $\bar{p}^{min}$; i.e. the curve consists on one unstable branch and another stable. Sufficiently high inflation accelerations transform the bijection of the static case into $\bar{p} - \lambda$ curves with an unstable portion.

- Neo-Hookean model: for $\ddot{\lambda} = 10$ the inflation curve does not show either a local maximum nor a local minimum, i.e. the curve consists on only one unstable branch. For $\ddot{\lambda} = 4$ and $\ddot{\lambda} = 2$ the inflation curve shows a maximum; i.e. the curve consists on one stable branch and another unstable.

- Yeoh model: for $\ddot{\lambda} = 10$ the inflation curve shows a local minimum $\bar{p}^{min}$; i.e. the curve consists on one unstable branch and another stable. For $\ddot{\lambda} = 4$ and $\ddot{\lambda} = 2$ the inflation curve shows a local maximum $\bar{p}^{max}$ and a local minimum $\bar{p}^{min}$; i.e. the curve consists on two stable branches and one unstable.

From previous analysis the following conclusions can be drawn: in comparison with static inflation, dynamic inflation at constant acceleration (1) boosts the inflation pressure and (2) dramatically changes the shape of the $\bar{p} - \lambda$ curves.

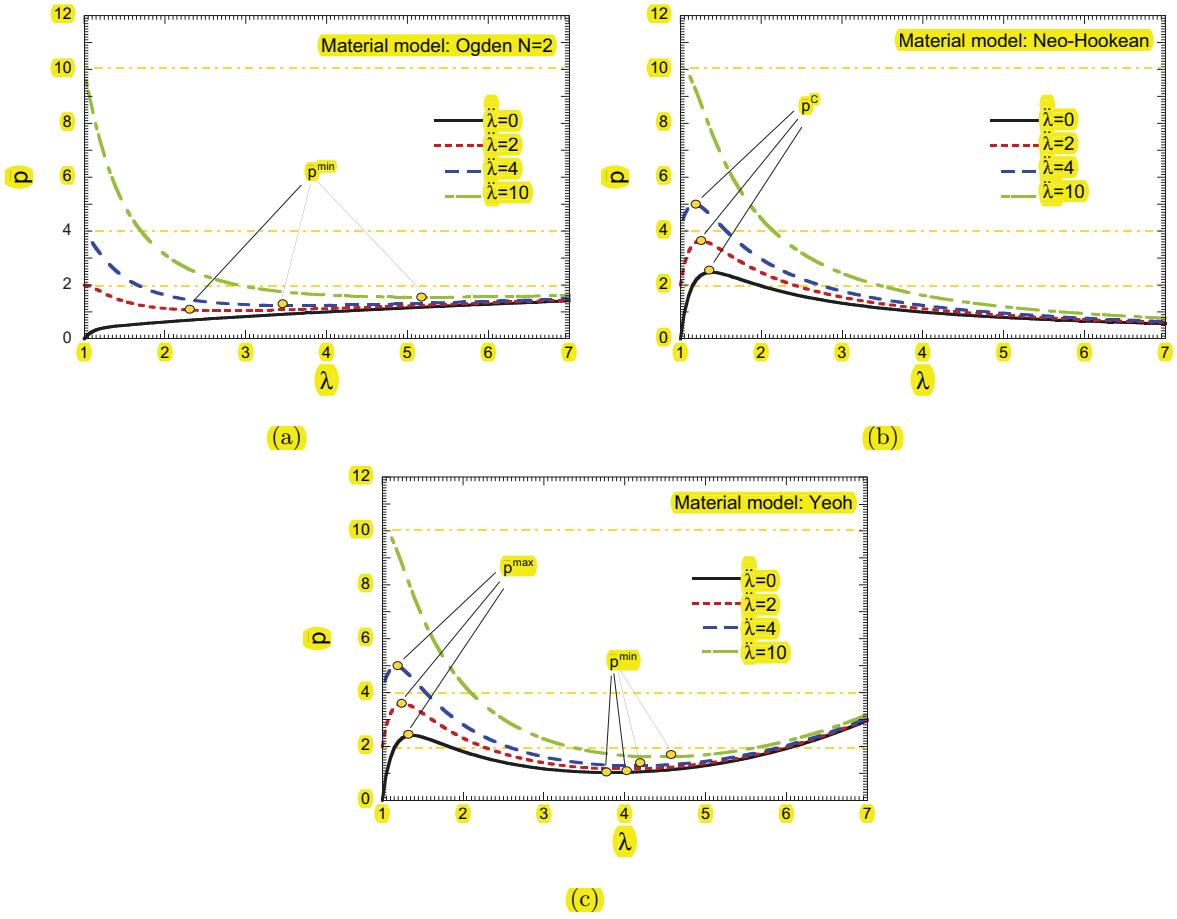

Figure 1: Dimensionless pressure $\bar{p}$ versus the circumferential stretch λ for several values of the acceleration $\ddot{\lambda}$. (a) Ogden N=2 model. (b) Neo-Hookean model. (c) Yeoh model.

4.1.2. Influence of strain-energy function

Next, we pay specific attention to the role that the strain-energy function has on the dynamic response of the membrane. Fig. 2 shows the dimensionless pressure $\bar{p}$ versus the circumferential stretch λ for two different accelerations and the six different strain-energy functions listed in

section 3. Irrespective of the acceleration considered, the inflation curve strongly depends on the strain-energy function. This relationship of dependence is such that, for given loading conditions, different constitutive models may trigger largely different *(distinctive)* predictions of the dynamic response of the membrane, as shown in Fig. 2. The $\bar{p} - \lambda$ curve may drastically change with the strain-energy function, and therefore the conditions of stability/instability of the membrane may do also. Illustrative examples are shown for $\ddot{\lambda} = 1$ and $\ddot{\lambda} = 15$:

- $\ddot{\lambda} = 1$: (1) For Neo-Hookean, Mooney-Rivlin and Ogden N=1 models the inflation curves show a maximum, i.e. the curves consist on one stable branch and one unstable. (2) For Yeoh, Ogden N=2 and Ogden N=3 models the inflation curves show a local maximum $\bar{p}^{max}$ and local minimum $\bar{p}^{min}$; i.e. the curves consist on two stable branches (the first one for Ogden N=2 is very short) and one unstable.
- $\ddot{\lambda} = 15$: (1) For Neo-Hookean, Mooney-Rivlin and Ogden N=1 models the inflation curves do not show either a maximum nor a minimum, i.e. the curves consist on only one unstable branch. (2) For Yeoh, Ogden N=2 and Ogden N=3 models the inflation curves show a local minimum $\bar{p}^{min}$; i.e. the curves consist on one unstable branch and another one stable.

The significance of these observations comes from the fact that, as mentioned before, the same experimental data were used to obtain the material parameters for the six strain-energy functions considered. Thus, the following conclusion can be drawn: the choice of the strain-energy function determines the dynamic response of the membrane up to an extent that (1) constitutive models calibrated using the same experimental data provide, for the same loading conditions, drastically different inflation curves which (2) strongly affects the conditions of stability/instability of the membrane.

4.2. Constant inflation pressure step

Loading case II (section 2.2.2) is addressed. Firstly, the role of inflation pressure on the response of the spherical membrane is explored.

4.2.1. Influence of inflation pressure step

Similarly to as section 4.1.1 is developed, Ogden N=2, Neo-Hookean and Yeoh models are selected to examine the influence of inflation pressure on the dynamic response of the membrane.

We first inspect the conditions for an oscillatory (stable) response. As discussed in section 2.2.2, when the motion of the membrane is periodic the corresponding phase curve is a closed

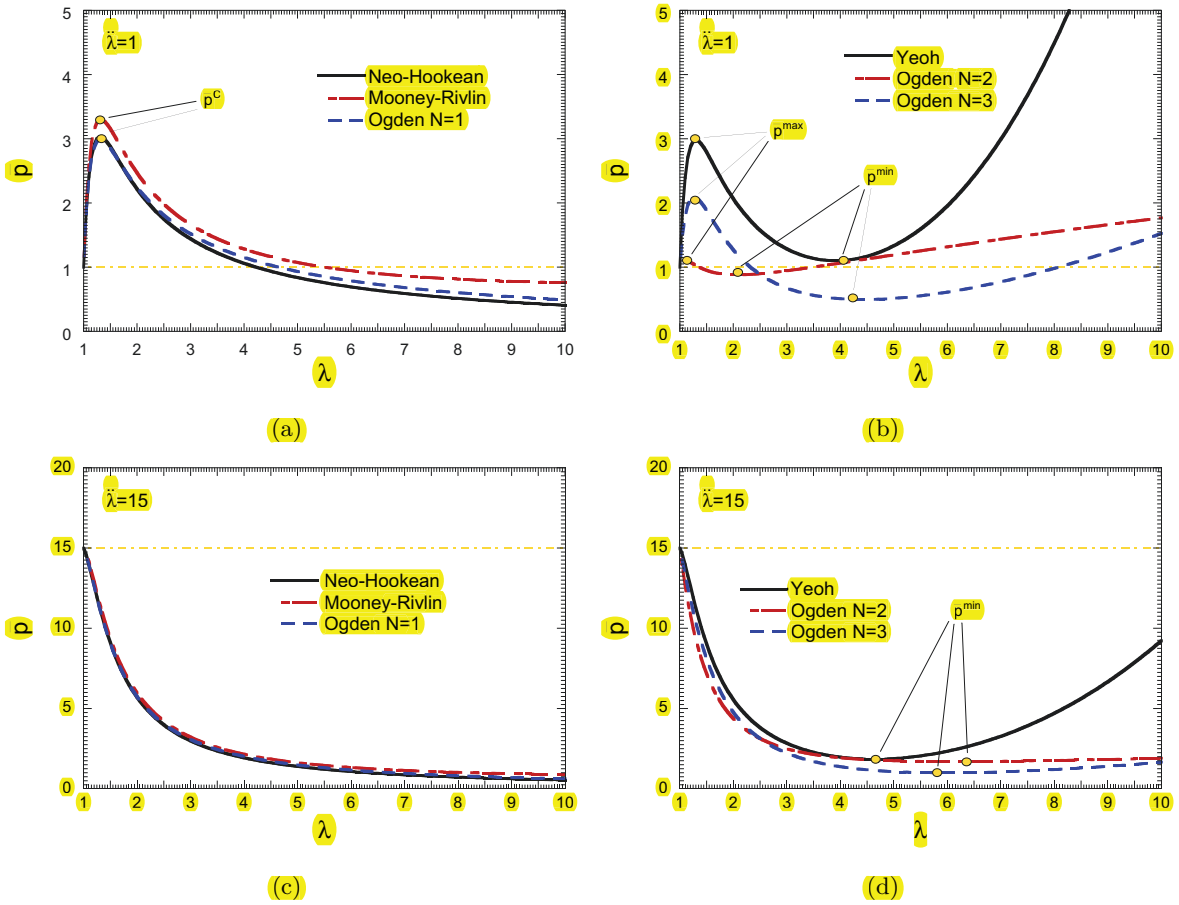

Figure 2: Dimensionless pressure $\bar{p}$ versus the circumferential stretch λ. (a) $\ddot{\lambda} = 1$, Neo-Hookean, Mooney-Rivlin and Ogden N=1 models. (b) $\ddot{\lambda} = 1$, Yeoh, Ogden N=2 and Ogden N=3 models. (c) $\ddot{\lambda} = 15$, Neo-Hookean, Mooney-Rivlin and Ogden N=1 models. (d) $\ddot{\lambda} = 15$, Yeoh, Ogden N=2 and Ogden N=3 models.

loop in the $(\lambda, \dot{\lambda})$ plane. The initial conditions $(1, 0)$ given by expression (6) define an intersection between the λ axis and the phase trajectory, therefore this trajectory must intersect the λ axis at least one more time for it to be a closed loop. If we set $\dot{\lambda} = 0$ in Eq. (10) we obtain this second intersection of the phase trajectory with the λ axis. Hereinafter this stretch value will be denoted as $\lambda|_{\dot{\lambda}=0}$.

Thus, Fig. 3 shows the comparison between static ($\dot{\lambda} = 0, \ddot{\lambda} = 0$) and dynamic ($\dot{\lambda} = 0, \ddot{\lambda} \neq 0$) inflations for the three strain-energy functions mentioned above. It has to be noted that the shape of the $\bar{p} - \lambda|_{\dot{\lambda}=0}$ dynamic curves is analogous to the shape of the $\bar{p} - \lambda|_{\dot{\lambda}=0}$ static curves (the latter have been previously denoted as $\bar{p} - \lambda$ in Fig. (1)). Besides that, a number of key points have to be highlighted:

- Ogden N=2 model: The dynamic inflation curve goes below the static one, irrespective of the value of $\lambda|_{\dot{\lambda}=0}$.
- Neo-Hookean model: The dynamic inflation curve goes below the static one until a maximum in the dynamic curve, $\bar{p}_d^c$, is reached. From that point on, the static inflation curve goes below the dynamic one.
- Yeoh model: The dynamic inflation curve goes below the static one until a relative maximum in the dynamic curve, $\bar{p}_d^{max}$, is reached. Then, the dynamic curve goes above the static one until a local minimum in the dynamic curve, $\bar{p}_d^{min}$, is reached. From that point on, the dynamic inflation curve goes below the static one.

Previous observations can be summarized as follows: the stable (oscillatory) portions of the dynamic inflation curves run below the static curves, whereas the unstable portions run above. In comparison with static inflation, dynamic inflation at constant pressure reduces the pressure that the membrane holds under stable conditions of deformation. In other words, for given loading pressure, the membranes experiences greater stretching under dynamic conditions. Note that the so-called physically unacceptable regions of Fig. 3 are such for the initial conditions that we have taken $\lambda(0) = 1$, $\dot{\lambda}(0) = 0$.

Next, in Fig. 4 we examine the phase diagrams, $\dot{\lambda}$ versus λ, obtained from Eq. (10) for three selected values of the inflation pressure, namely $\bar{p} = 2$, $\bar{p} = 4$ and $\bar{p} = 6$. In the first shot of the analysis, we will comment separately on the three constitutive models considered in this section.

- Ogden N=2 model: The phase diagram is a closed loop, Fig. 4(a), i.e. the membrane

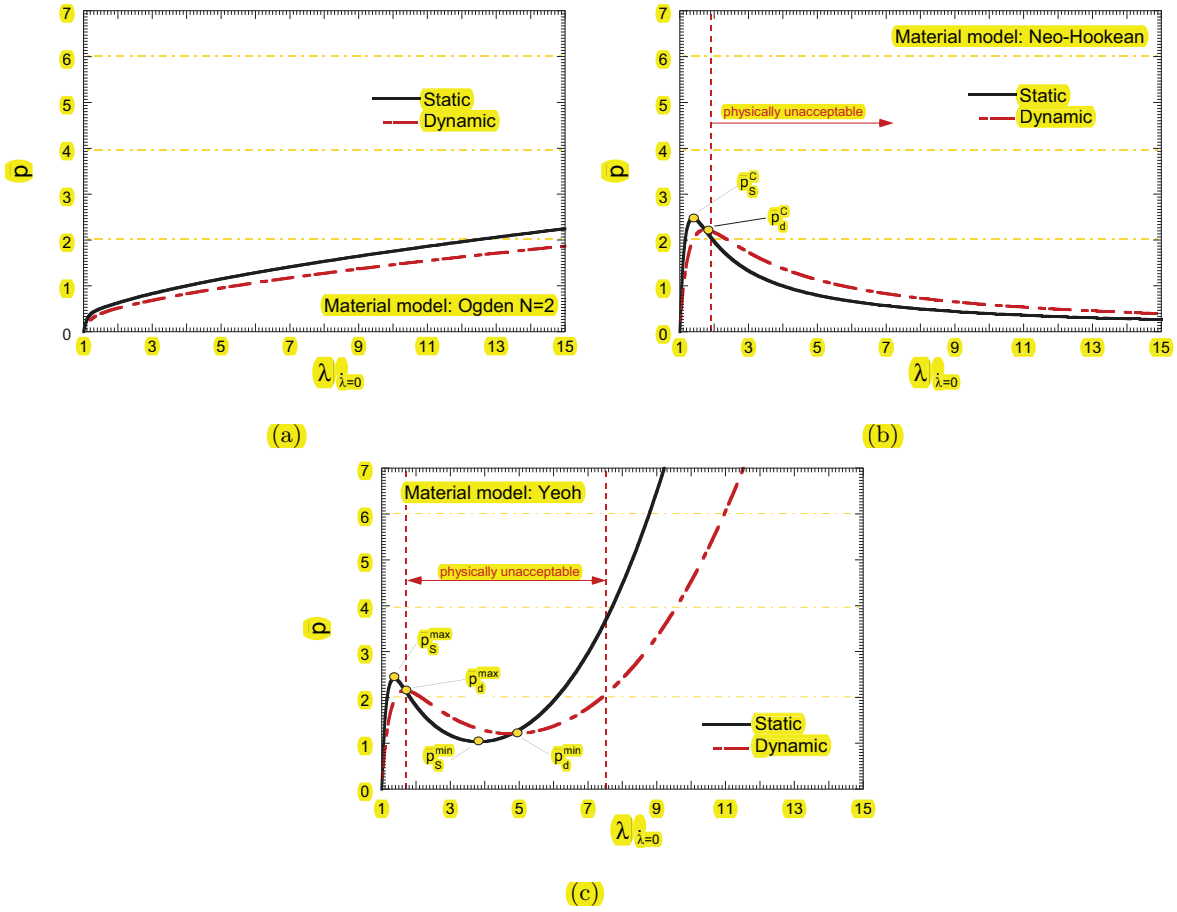

Figure 3: Dimensionless pressure $\bar{p}$ versus the circumferential stretch $\lambda|_{\dot{\lambda}=0}$ for static and dynamic inflations. (a) Ogden N=2 model. (b) Neo-Hookean model. (c) Yeoh model. Note that the physically unacceptable regions are such for the initial conditions that we have taken $\lambda(0) = 1$, $\dot{\lambda}(0) = 0$.

shows a periodic (stable) response irrespective of the inflation pressure. This is because the dynamic inflation curve $\bar{p}-\lambda|_{\dot{\lambda}=0}$ is a bijection (see Fig. 3(a)). For a given inflating pressure $\bar{p}$, the membrane oscillates between the initial condition $(1,0)$ and the maximum stretch $(\lambda_{max},0)$. The latter is represented in Fig. 3(a) by the intersection point of the dynamic inflating curve with the corresponding pressure level. As deduced from Fig. 3(a) the value of λ_{max} increases with $\bar{p}$. Interestingly, larger stretch rates $\dot{\lambda}$ are also obtained increasing $\bar{p}$. In other words, as the inflation pressure increases the membrane stretches more and faster.

- Neo-Hookean model: For $\bar{p}=2$ we have that the applied pressure is smaller than $\bar{p}_d^c$, Fig. 4(b), as we can observe in Fig. 3(b). The phase diagram is split into two parts. (1) The first part is a closed loop which describes an oscillation of the membrane between the initial condition $(1,0)$ and the maximum stretch $(\lambda_{max},0)$. The latter is represented in Fig. 3(b) by the first intersection point of the dynamic inflating curve with the pressure level $\bar{p}=2$. (2) The second part is an open curve which describes an unstable response of the membrane. Let us note the origin of the curve as $(\lambda_u,0)$, this is represented in Fig. 3(b) by the second intersection point of the dynamic inflating curve with the pressure level $\bar{p}=2$. Therefore, this behaviour is not physically acceptable for a membrane initially in equilibrium and unstretched, i.e. subjected to the initial conditions defined by expression (6). Physically, the membrane cannot reach the stretch value λ_u for a $\bar{p}<\bar{p}_d^c$. For $\bar{p}=4$ and $\bar{p}=6$ the applied pressure is greater than $\bar{p}_d^c$, as we can observe in Fig. 3(b). In other words, the applied pressure is larger than the maximum pressure that the membrane can withstand. The phase diagram is an open curve whose origin is given by the initial conditions defined by expression (6).

- Yeoh model: For $\bar{p}=2$ we have that the applied pressure is smaller than $\bar{p}_d^{max}$, Fig. 4(c), as we can observe in Fig. 3(c). The phase diagram is split into two parts. (1) A closed loop which describes a periodic response of the membrane between the initial condition $(1,0)$ and the maximum stretch $(\lambda_{max},0)$. The latter corresponds in Fig. 3(c) with the first intersection point of the dynamic inflating curve with the pressure level $\bar{p}=2$. To be noted that this intersection point is located in the first stable branch of the inflating curve. (2) A closed curve which, according to those comments reported in previous paragraph for the Neo-Hookean model, is not physically acceptable for a membrane initially in equilibrium and unstretched. The membrane cannot reach the stretch value λ_u for $\bar{p}<\bar{p}_d^{max}$. For $\bar{p}=4$

and $\bar{p} = 6$ the applied pressure is greater than $\bar{p}_d^{max}$, as we can observe in Fig. 3(c). The phase diagram is a closed loop which represents an oscillatory response of the membrane between the initial conditions given by expression (6) and the maximum stretch $(\lambda_{max}, 0)$. The latter is located in the second stable portion of the dynamic inflating curve represented in Fig. 3(c). It has to be noted that the values of λ_{max} and $\dot{\lambda}$ which characterize the oscillatory response of the membrane drastically increase if $\bar{p} > \bar{p}_d^{max}$.

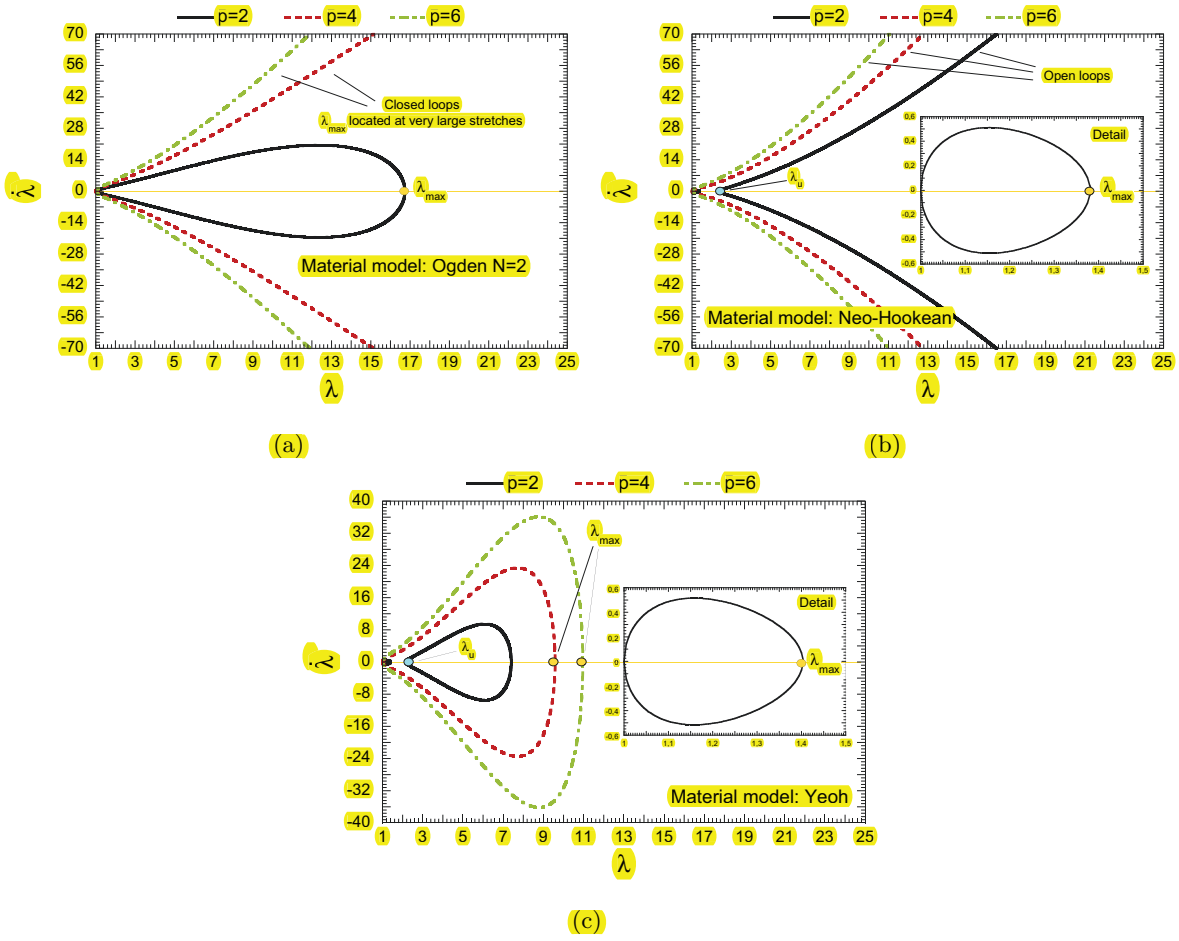

Figure 4: Phase diagrams, $\dot{\lambda}$ versus λ, for three selected values of the inflation pressure, namely $\bar{p} = 2$, $\bar{p} = 4$ and $\bar{p} = 6$. (a) Ogden N=2 model. (b) Neo-Hookean model. (c) Yeoh model.

From previous analysis, we can deduce that: increasing inflating pressure boosts the maximum stretch and stretch rate up to an extent that, for certain constitutive models, the response of the membrane may turn from stable (oscillatory) to unstable.

We continue by showing in Fig. 5 the period of motion as a function of the inflating pressure, T versus $\bar{p}$, obtained from Eq. (12) for the same constitutive models considered before.

- Ogden N=2 model: Firstly the period increases with $\bar{p}$, then it reaches a maximum denoted in Fig. 5 by T_{max}, finally it decreases monotonically with $\bar{p}$. The maximum comes from achieving an *optimum* balance between the raise of λ_{max} with $\bar{p}$, which tends to increase the period, and the raise of $\dot{\lambda}$ with $\bar{p}$, which tends to decrease the period.

- Neo-Hookean model: The period of motion continuously increases with $\bar{p}$. When the applied pressure reaches $\bar{p}_d^c$, the membrane becomes unstable and we obtain that $T \to \infty$. The oscillatory character of the membrane response is lost.

- Yeoh model: Firstly the period increases with $\bar{p}$. When the applied pressure reaches $\bar{p}_d^{max}$, the membrane tends to reach an unstable static (non-oscillatory) equilibrium and $T \to \infty$. For $\bar{p} > \bar{p}_d^{max}$ the membrane oscillates again and the period decreases monotonically with $\bar{p}$.

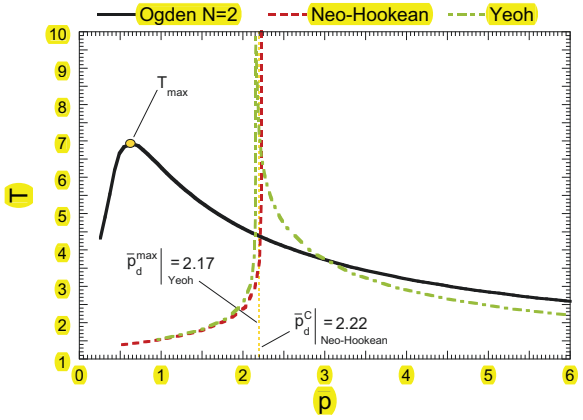

Figure 5: Period of motion as a function of the inflating pressure, T versus $\bar{p}$, for the three selected strain-energy functions, namely: Ogden N=2, Neo-Hookean and Yeoh models. Since $\bar{p}_d^{max}\,|_{Yeoh} \approx \bar{p}_d^c\,|_{Neo-Hookean}$ only a vertical line is drawn in the graph for the sake of clarity.

It becomes clear that, irrespective of the constitutive model, the period of motion does not increase monotonically with inflating pressure.

4.2.2. Influence of strain-energy function

Next, we pay specific attention to the role that the strain-energy function has on the dynamic response of the membrane. For that task, we use here the six different strain-energy functions listed in section 3.

We first inspect the conditions for an oscillatory response. Fig. 6 shows the dynamic inflation

curves, $\bar{p}$ versus $\lambda|_{\dot{\lambda}=0}$. It has to be highlighted the impact that the strain energy function has on the dynamic inflation curve. Namely:

- Neo-Hookean, Mooney-Rivlin and Ogden N=1 models: the dynamic inflation curve firstly shows a stable branch up to $\bar{p} = \bar{p}_d^c$, beyond this value of applied pressure the membrane becomes unstable.

- Yeoh and Ogden N=3 models: the dynamic inflation curve firstly shows a stable branch up to $\bar{p} = \bar{p}_d^{max}$, subsequently the curve becomes unstable until $\bar{p} = \bar{p}_d^{min}$ and beyond this value of applied pressure the membrane becomes stable again (although the curve becomes stable, it is physically unacceptable if $\bar{p} < \bar{p}_d^{max}$ for the initial conditions that we have selected $\lambda(0) = 1$, $\dot{\lambda}(0) = 0$).

- Ogden N=2 model: the dynamic inflation curve is stable no matter the value of the applied pressure.

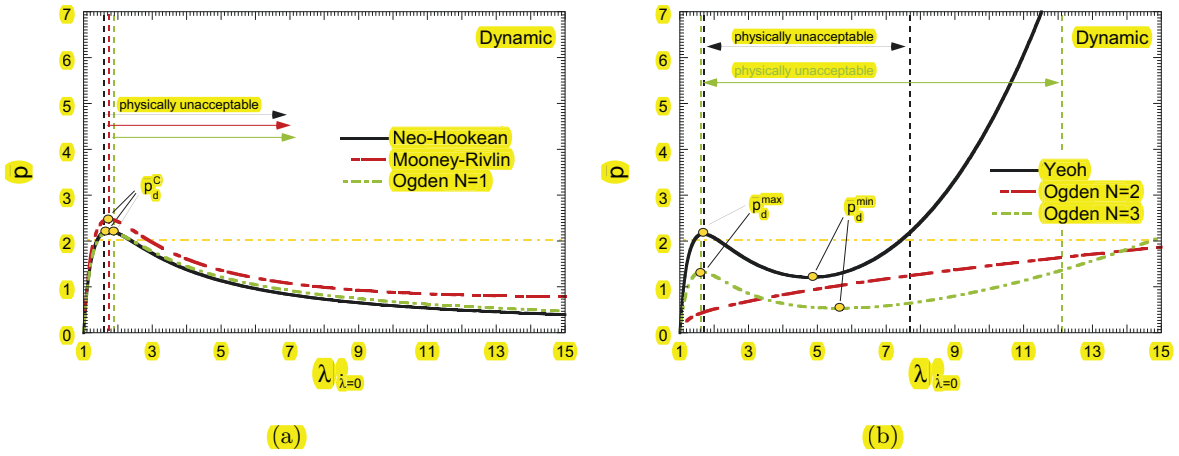

Figure 6: Dimensionless pressure $\bar{p}$ versus the circumferential stretch $\lambda|_{\dot{\lambda}=0}$. (a) Neo-Hookean, Mooney-Rivlin and Ogden N=1 models. (b) Yeoh, Ogden N=2 and Ogden N=3 models. Note that the physically unacceptable regions are such for the initial conditions that we have selected $\lambda(0) = 1$, $\dot{\lambda}(0) = 0$.

The main outcome of this part of the analysis is to reinforce an idea previously introduced in this paper: constitutive models calibrated using the same experimental data can lead to very different stability/instability conditions for the membrane. While this conclusion was obtained in section 4.1.2 for the case of constant acceleration, here this statement has been extended to the case of constant pressure.

Next, in Fig. 7 we show the phase diagrams obtained for $\bar{p} = 2$. This is a very illustrative example since we can observe very distinct responses of the membrane within the six constitutive models used, namely:

- Neo-Hookean, Mooney-Rivlin and Ogden N=1: We find that the applied pressure is smaller than $\bar{p}_d^c$, as we can observe in Fig. 6. The phase diagram is split into two parts, a closed loop and an open loop. Only the closed loop which describes an oscillation of the membrane between the initial condition $(1, 0)$ and the maximum stretch $(\lambda_{max}, 0)$ has physical meaning.

- Yeoh model: The applied pressure is smaller than $\bar{p}_d^{max}$, as shown in Fig. 6. The phase diagram is split into two closed loops. Only the portion which describes an oscillation of the membrane between the initial condition $(1, 0)$ and the maximum stretch $(\lambda_{max}, 0)$ has physical meaning.

- Ogden N=2: The phase diagram is a closed loop, i.e. the membrane shows a periodic response. The membrane oscillates between the initial conditions $(1, 0)$ and the maximum stretch $(\lambda_{max}, 0)$.

- Ogden N=3: We find that the applied pressure is greater than $\bar{p}_d^{max}$, as we can observe in Fig. 6(b). The phase diagram represents an oscillatory response of the membrane between the initial conditions $(1, 0)$ and the maximum stretch $(\lambda_{max}, 0)$. The latter point is located in the second stable portion of the dynamic inflating curve.

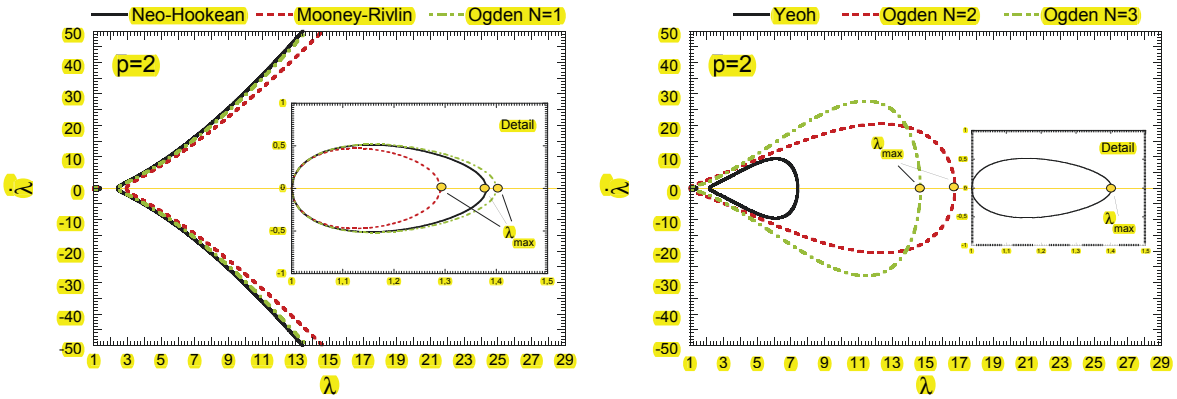

(a) (b)

Figure 7: Phase diagrams, $\dot{\lambda}$ versus λ, for $\bar{p} = 2$. (a) Neo-Hookean, Mooney-Rivlin and Ogden N=1 models. (b) Yeoh, Ogden N=2 and Ogden N=3 models.

Furthermore, we observe that the constitutive relation not only acts upon the maximum stretch λ_{max}, but it also largely affects to the stretch rate $\dot{\lambda}$. Let us stress again that the constitutive model exerts great influence on how much and how fast the membrane deforms.

This idea can be further discussed relying on Fig. 8, where we show the period of motion obtained from Eq. (12) as a function of the inflating pressure. We can observe three distinct responses of the membrane within the six constitutive models used, namely:

- Neo-Hookean, Mooney-Rivlin and Ogden N=1 models: For these three strain-energy functions the period increases monotonically with $\bar{p}$ up to $\bar{p} = \bar{p}_d^c$. Then, $T \to \infty$ which illustrates that the inflating pressure has reached the maximum pressure that the membrane can withstand. Within the ranges of inflating pressures for which the membrane oscillates, irrespective of the constitutive relation considered, the relationship $T - \bar{p}$ is highly dependent on the constitutive model. Namely, T is markedly smaller for Mooney-Rivlin than for Ogden N=1 and Neo-Hookean models.

- Yeoh and Ogden N=3 models: For these two strain-energy functions the period increases monotonically with $\bar{p}$ up to $\bar{p} = \bar{p}_d^{max}$. Then, $T \to \infty$ which illustrates that the membrane has reached an unstable (static) equilibrium. Further increase of inflating pressure implies that the membrane retrieves an oscillatory behaviour. Then, the period of motion monotonically decreases with increasing inflating pressure. The curves $T - \bar{p}$ are found highly sensitive to the strain-energy function. In particular, within the lower range of inflating pressures considered, T is much greater for Ogden N=3 model than for Yeoh model.

- Ogden N=2: For this model it was already commented in section 4.2.1 of this paper that firstly the period increases with $\bar{p}$, then it reaches a maximum and finally it decreases monotonically with $\bar{p}$. Unlike the rest of the models analysed, the curve $T - \bar{p}$ is smooth and does not show any excursion within the inflating pressures analysed.

We show here the great impact of the strain-energy function on the dynamic behaviour of the membrane response. The period of oscillation, in case we assume loading conditions for which the membrane oscillates, is largely controlled by the strain-energy function.

5. Discussion

The present paper provides an analytical investigation on the role that the constitutive model has on the stability of hyper-elastic spherical membranes subjected to dynamic inflation. Two

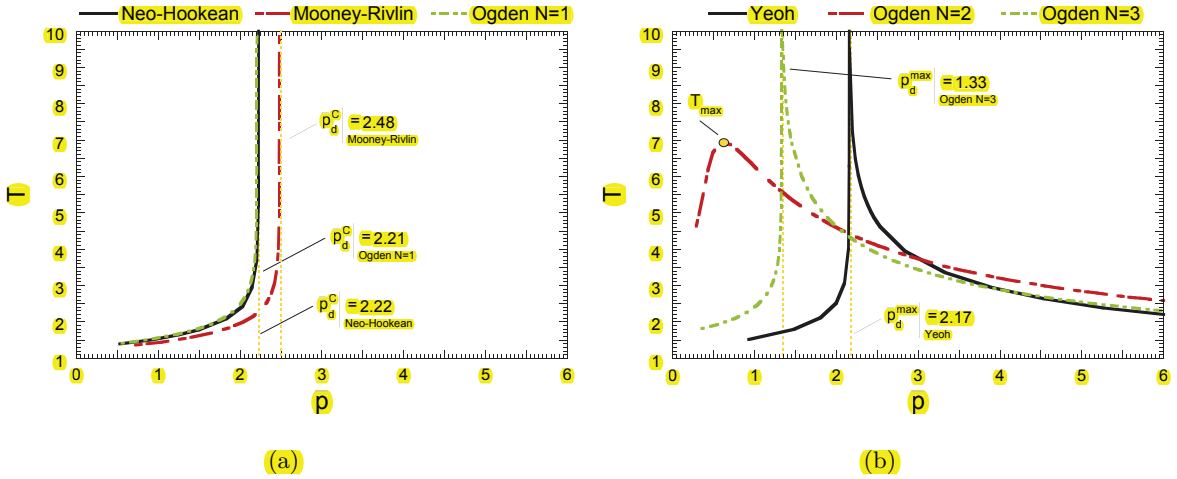

Figure 8: Period of motion T as a function of the inflating pressure $\bar{p}$. (a) Neo-Hookean, Mooney-Rivlin and Ogden N=1 models. (b) Yeoh, Ogden N=2 and Ogden N=3 models. Since $\bar{p}_d^c\,|_{Neo-Hookean} \approx \bar{p}_d^c\,|_{OgdenN=1}$ only a vertical line for both models is drawn in Fig. 8(a) for the sake of clarity.

distinctive loading scenarios are addressed: (1) constant inflation acceleration and (2) constant inflation pressure step. Besides that, six different strain-energy functions are investigated: three of the Mooney-Rivlin class and three of the Ogden class. Results are presented combining, systematically, the two loading scenarios and the six constitutive equations. In this regard, we present here an analysis on the dynamic response of elastomeric spherical shells with unprecedented scope in this field. As such, the outcomes of this study show the great influence of the constitutive model on the mechanical stability of rubber-like balloons subjected to dynamic loading. The interest of this observation relies on the fact that the constitutive models were calibrated using the same set of experimental data and the same fitting procedure (Bucchi and Hearn, 2013a,b). We observe that the oscillatory (stable) response of the membrane is highly conditioned by the strain-energy function selected. Furthermore, whenever the membrane oscillates, the characteristics of the oscillation differ pretty much from one constitutive model to another. We emphasize that the strain-energy function dictates, at a large extent, how much and how fast the membrane deforms.

In this regard, we show a need to reduce the uncertainty surrounding the dynamic constitutive modelling of rubber-like materials. This task has to be accomplished by developing new experiments which allow to obtain reliable data on the mechanical behaviour of rubber-like materials at large strains and high strain rates. On the one hand, mechanical testing at large strains is required to explore strain-driven instabilities. On the other hand, mechanical testing at high strain rates shall allow to uncover the specific role that rate effects may have on the dynamic

Neo-Hookean parameters, Eq. (14)	
C_{10}^{M1} $[Pa]$	191999.034

Table A.1: Neo-Hookean parameters, Eq. (14).

Mooney-Rivlin parameters, Eq. (15)	
C_{10}^{M2} $[Pa]$	210587.307
C_{01}^{M2} $[Pa]$	1504.76719

Table A.2: Mooney-Rivlin parameters, Eq. (15).

response of the material. Namely, we have to further understand the impact that rate effects may have on boosting/damping strain-driven instabilities. Any step in this direction will help to derive more reliable constitutive models of hyper-elastic materials.

6. Concluding remarks

We developed in this paper a theoretical analysis to explore the response of thin-walled spherical shells subjected to dynamic inflation. It has been highlighted the fundamental role that the constitutive relation selected to describe the membrane materials has on the outcomes of our modelling. The key point here is that the constitutive models considered were calibrated using the same set of experimental data and the same fitting procedure. We claim that success of mathematical models as a tool to understand and predict the processes of enlargement and rupture of this type of elastomeric shell structures is closely related to the constitutive description of the material.

Appendix A. Material parameters of the strain-energy functions

We show below the material parameters used in the constitutive models listed in section 3. They are all taken from Bucchi and Hearn (2013b).

Yeoh parameters, Eq. (16)	
C_{10}^{M3} $[Pa]$	190592.559
C_{20}^{M3} $[Pa]$	−1634.89996
C_{30}^{M3} $[Pa]$	41.3399927

Table A.3: Yeoh parameters, Eq. (16).

Ogden N=1 parameters, Eq. (18)	
C_{10}^{O1} $[Pa]$	359237.938
α_1^{O1}	2.11120130

Table A.4: Ogden N=1 parameters, Eq. (18).

Ogden N=2 parameters, Eq. (19)	
C_{10}^{O2} $[Pa]$	42073.4586
C_{20}^{O2} $[Pa]$	360636.118
α_1^{O2}	3.60405498
α_2^{O2}	−0.03270528

Table A.5: Ogden N=2 parameters, Eq. (19).

Ogden N=3 parameters, Eq. (20)	
C_{10}^{O3} $[Pa]$	398206.801
C_{20}^{O3} $[Pa]$	5377.71517
C_{30}^{O3} $[Pa]$	7647.41545
α_1^{O3}	1.13176086
α_2^{O3}	4.73211925
α_3^{O3}	-2.14619240

Table A.6: Ogden N=3 parameters, Eq. (20).

References

Alhayani, A. A., Rodríguez, J., J., M., 2014. Competition between radial expansion and axial propagation in bulging of inflated cylinders with application to aneurysms propagation in arterial wall tissue. International Journal of Engineering Science 85, 74–89.

Beatty, M. F., 1987. Topics in Finite Elasticity: Hyperelasticity of Rubber, Elastomers, and Biological Tissues - With Examples. Applied Mechanics Reviews 40, 1699–1734.

Beatty, M. F., 2009. Small amplitude radial oscillations of an incompressible, isotropic elastic spherical shell. Mathematics and Mechanics of Solids 16, 492–512.

Biscari, P., Omati, C., 2010. Stability of generalized Knowles solids. IMA Journal of Applied Mathematics 75, 479–491.

Bucchi, A., Hearn, E. H., 2013a. Predictions of aneurysm formation in distensible tubes: Part A - Theoretical background to alternative approaches. International Journal of Mechanical Sciences 71, 1–20.

Bucchi, A., Hearn, E. H., 2013b. Predictions of aneurysm formation in distensible tubes: Part B - Application and comparison of alternative approaches. International Journal of Mechanical Sciences 70, 155–170.

David, G., Humphrey, J. D., 2003. Further evidence for the dynamic stability of intracranial saccular aneurysms. Journal of Biomechanics 36, 1143–1150.

Destrade, M., Annaidh, A. N., Ciprian, D. C., 2009. Bending instabilities of soft biological tissues. International Journal of Solids and Structures 46, 4322–4330.

Freitas, P., 2009. On the effect of sharp rises in blood pressure in the Shah–Humphrey model for intracranial saccular aneurysms. Biomechanics and Modeling in Mechanobiology 8, 457–471.

Fu, Y. B., Pearce, S. P., Liu, K. K., 2008. Post-bifurcation analysis of a thin-walled hyperelastic tube under inflation. International Journal of Non-Linear Mechanics 43, 697–706.

Fu, Y. B., Rogerson, G. A., Zhang, Y. T., 2012. Initiation of aneurysms as a mechanical bifurcation phenomenon. International Journal of Non-linear Mechanics 47, 179–184.

Fu, Y. B., Xie, Y. X., 2010. Stability of localized bulging in inflated membrane tubes under volume control. International Journal of Engineering Science 48, 1242–1252.

Fu, Y. B., Xie, Y. X., 2012. Effects of imperfections on localized bulging in inflated membrane tubes. Philosophical Transactions of the Royal Society: Mathematical, Physical and Engineering Sciences 370, 1896–1911.

Fu, Y. B., Xie, Y. X., 2014. Stability of pear-shaped configurations bifurcated from a pressurized spherical balloon. Journal of the Mechanics and Physics of Solids 68, 33–44.

Haslach, H., Humphrey, J. D., 2004. Dynamics of biological soft tissue and rubber: internally pressurized spherical membranes surrounded by a fluid. International Journal of Non-Linear Mechanics 39, 399–420.

Hoo Fatt, M. S., Ouyang, X., 2008. Three-dimensional constitutive equations for Styrene Butadiene Rubber at high strain rates. Mechanics of Materials 40, 1–16.

Il'ichev, A. T., Fu, Y. B., 2012. Stability of aneurysm solutions in a fluid-filled elastic membrane tube. Acta Mechancia Sinica 28, 1209–1218.

Il'ichev, A. T., Fu, Y. B., 2014. Stability of an inflated hyperelastic membrane tube with localized wall thinning. International Journal of Engineerigng Science 80, 53–61.

Janele, P., Haddow, J. B., Mioduchowski, A., 1989. Finite amplitude spherically symmetric wave propagation in a compressible hyperelastic solid. Acta Mechanica 79, 25–41.

Knowles, J. K., 1977. The finite anti-plane shear field near the tip of a crack for a class of incompressible elastic solids. International Journal of Fracture 13, 611–639.

Kumar, N., DasGupta, A., 2013. On the contact problem of an inflated spherical hyperelastic membrane. International Journal of Non-Linear Mechanics 57, 130–139.

Mangan, R., Destrade, M., 2015. Gent models for the inflation of spherical balloons. International Journal of Non-Linear Mechanicss 68, 52–58.

Mooney, M., 1940. A Theory of Large Elastic Deformation. Journal of Applied Physics 11, 582–592.

Ogden, R. W., 1972. Large deformation isotropic elasticity – on the correlation of theory and experiment for incompressible rubber-like solids. Proceedins Royal Society of London 326, 565–584.

Ogden, R. W., 1997. Non-linear elastic deformations. Dover Publications, Mineola (N.Y.).

Ogden, R. W., Saccomandi, G., 2007. Introducing mesoscopic information into constitutive equations for arterial walls. Biomechanics and Modeling in Mechanobiology 6, 333–344.

Ogden, R. W., Saccomandi, G., Sgura, I., 2004. Fitting hyperelastic models to experimental data. Computational Mechanics 34, 484–502.

Pearce, S. P., Fu, Y. B., 2010. Characterization and stability of localized bulging/necking in inflated membrane tubes. IMA Journal of Applied Mathematics 75, 581–602.

Pucci, E., Saccomandi, G., 2002. A note on the Gent model for rubber-like materials. Rubber Chemistry and Technology 75, 839–851.

Rivlin, R. S., 1948. Large elastic deformations of isotropic materials. Philosophical Transactions of the Royal Society A240, 459–491.

Rivlin, R. S., 1996. Collected Papers of R. S. Rivlin, Editors: Barenblatt, G. I. and Joseph, D. D. Edition. Springer.

Rodríguez, J., Merodio, J., 2011. A new derivation of the bifurcation conditions of inflated cylindrical membranes of elastic material under axial loading. Application to aneurysm formation. Mechanics Research Communications 38, 203–210.

Shah, A. D., Humphrey, J. D., 1999. Finite strain elastodynamics of saccular aneurysms. Journal of Biomechanics 32, 593–599.

Tamadapu, G., DasGupta, A., 2013. Finite inflation analysis of a hyperelastic toroidal membrane of initially circular cross-section. International Journal of Non-Linear Mechanics 49, 31–39.

Treolar, L. R. G., 1944. Stress–strain data for vulcanised rubber under various types of deformation. Transactions of the Faraday Society 40, 59–70.

Treolar, L. R. G., 1949. The physics of rubber elasticity. Clarendon Press, Oxford, UK.

Verron, E., Khayat, R. E., Derdouri, A., Peseux, B., 1999. Dynamic inflation of hyperelastic spherical membranes. Journal of Rheology 43, 1083–1097.

Verron, E., Marckmann, G., Peseux, B., 2001. Dynamic inflation of non-linear elastic and viscoelastic rubber-like membranes. International Journal for Numerical Methods in Engineering 50, 1233–1251.

Volokh, K. Y., 2011. Modeling failure of soft anisotropic materials with application to arteries. Journal of the Mechanical Behavior of Biomedical Materials 4, 1582–1594.

Volokh, K. Y., Vorp, D. A., 2008. A model of growth and rupture of abdominal aortic aneurysm. Journal of Biomechanics 41, 1015–1021.

Wolters, B. J. B. M., Rutten, M. C. M., Schurink, G. W. H., Kose, U., Hart, J., van de Vosse, F. N., 2005. Patient-specific computational model of fluid–structure interaction in abdominal aortic aneurysms. Medical Engineering & Physics 27, 871–883.

Yeoh, O. H., 1993. Some forms of the strain-energy function for rubber. Rubber Chemistry and Technology 66, 754–771.

Yuan, X.-G., Zhang, H.-W., Ren, J.-S., Zhu, Z.-Y., 2010. Some qualitative properties of incompressible hyperelastic spherical membranes under dynamic loads. Applied Mathematics and Mechanics 31, 903–910.